Journal of Polish CIMAC
Gdansk University of Technology
The Faculty of Ocean Engineering and Ship Technology

ELECTRODE VIBRATIONS SYNCHRONIZATION IN ELECTROCHEMICAL MACHINING

Tomasz Paczkowski

University of Technology and Life Sciences in Bydgoszcz
Faculty of Mechanical Engineering
al. Prof. S. Kaliskiego 7, 85-789 Bydgoszcz, Poland
tel.: +48 52 340-87-47, fax: +48 52 340-82-45
tel. 52 340-87-47
e-mail: tompacz@utp.edu.pl

Abstract

The article deals with a theoretical analysis of electrochemical machining using a tool electrode with curvilinear profile, vibrating into two directions.

Physical phenomena occurring within the interelectrode gap have been described by a partial differential equations resulting from the balance of mass, momentum and energy of the electrolyte flowing through the gap.

Equations formulated in the paper which describe the work-piece surface shape evolution and the electrolyte flow (mixture of fluid and gas) through the gap, were simplified by means of assumptions concerning the flow, distribution of the volume fracture, and the gap thickness Then, they were solved , in part analytically, and in part numerically. Calculations were performed for the assumed machining parameters, with presentation of the calculation results in the sections across and along the interelectrode gap.

In the charts, the electrolyte longitudinal and transverse flow rate distributions, pressure, temperature distributions and distributions of chosen physical quantities of the electrochemical machining machining are demonstrated for the considered case of electrode vibrations synchronization.

Keywords*: ECM machining, computer simulation, oscillating electrode*

1. Introduction

Current pace of development and market demands motivate people to introduce innovations and improve already existing products. This, in turn, results in creation of specialist modules and independent modelers for the design of objects based on free curvilinear surfaces modeling, e.g. of NURBUS type. Representation of NURBUS is the most universal representation form for curvilinear surfaces and surfaces for all applications in the field of CAD-CAM or computer graphic [4]. Mathematical description of these surfaces is quite complicated due to their being curvilinear which makes it difficult to model the processes occurring during ECM.

Apart from the electrode geometry determination , the choice of the electrolyte composition and the machining parameters is of great importance for the design of a technological machining process with the use of a curvilinear tool electrode.

During the constant process, the electrode usually performs translation in the direction of the machined surface. The electrolyte is supplied with relatively high velocity to the interelectrode gap causing that dissolution products are carried away from the interelectrode space.

Hydrodynamic parameters of the flow and properties of the medium determine the processes of mass, momentum and energy exchange within the interelectrode gap. Properly chosen, they prevent from formation of cavitation zones, critical flow, circulation, excessive rise of the electrolyte temperature and volume fracture [1,2]. The listed above processes are closely related to each other and they largely affect the shape and applicability of the machined surface [6,10,11].

Due to the machining accuracy the process should be performed with possibly small thickness of the interelectrode gap. With the use of constant current, decreasing the gap thickness is connected with the increase of volume fracture in the electrolyte and its temperature. Use of gaps smaller that 0,1mm is limited by possibilities of dissolution product removal from the machining area [9]. Introduction of the electrode tool vibrations results in changes of the interelectrode gap thickness during the process of machining which, with a minimal gap, allows for improvement of the machining accuracy. Whereas, with a maximum gap, there are created good conditions for the electrolyte exchange. The electrode vibrations induced into two directions improve the machining accuracy in all the directions normal for curvilinear surfaces. The electrode vibrations synchronization additionally influences the process conditions.

For the purpose of appropriate choice of the process parameters and determination of the electrode geometry, mathematical modeling of phenomena occurring within the interelectrode gap is indispensable.

2. Mathematical modeling of the process

The purpose of modeling is a mathematical description of ECM process, which allows us to determine:

- the connection of the shape of the tool electrode (TE) and work piece (WP),
- the conditions in the inter-electrode gap (IEG),
- basic characteristics of the ECM process for vibrating electrodes.

For the considered curvilinear surfaces of the electrodes a superposition method of the obtained equations describing the two-dimensional electrolyte and hydrogen flow was used. The flow was considered in the local *xy*-system determined by the vector normal to the work electrode surface. The calculations were made for the consecutive xy surfaces defined along the *Z*-axis (Fig. 1). The coordinate systems were connected to the anode.

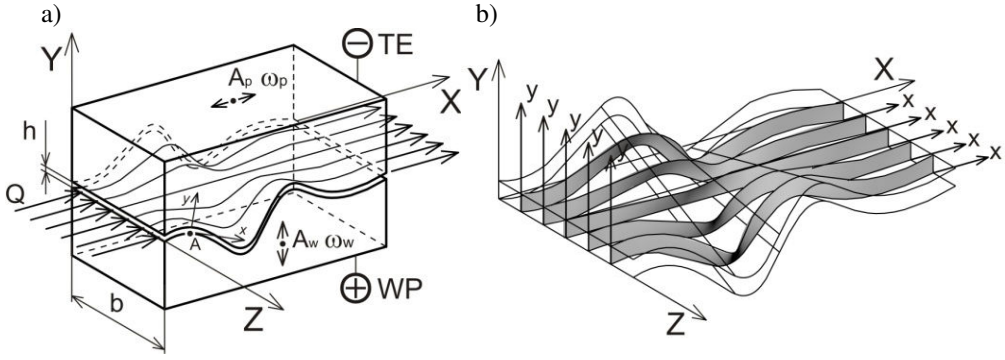

Fig. 1. Area flow of electrolyte in interelectrode gap: a) the shape of the electrodes, b) local coordinate system xy

The system of equations describing two-dimensional flow of the electrolyte and hydrogen through the interelectrode gap results from the principles of mass and momentum preservation [3].

Having introduced the following denotations:

- electrolyte flow is stable, two dimensional, homogenous,
- pressures $p_e = p_H = p$,
- volume fracture $\beta=\beta(x)$,
- the gap thickness is small compared to the interelectrode gap length ($h << L$),
- IEG power supplying with a constant volume flow of $Q=const$ electrolyte.

The equation system of the compound motion in the local orthogonal system of coordinates x,y connected with the anode (Fig. 1) is as follows:

$$\frac{\partial(\rho_e v_x)}{\partial x}+\frac{\partial(\rho_e v_y)}{\partial y}=0 \tag{1}$$

$$\frac{\partial(\rho_H v_x)}{\partial x}+\frac{\partial(\rho_H v_y)}{\partial y}=j\eta_H k_H h^{-1} \tag{2}$$

$$\rho_e\left(\frac{\partial v_x}{\partial t}+v_x\frac{\partial v_x}{\partial x}+v_y\frac{\partial v_x}{\partial y}\right)=-\frac{\partial p}{\partial x}+\mu_e\left(\frac{\partial^2 v_x}{\partial y^2}\right) \tag{3}$$

$$v_x\frac{\partial T}{\partial x}+v_y\frac{\partial T}{\partial y}=\frac{\partial}{\partial x}\left((a+a_T)\frac{\partial T}{\partial x}\right)+\frac{j^2}{\rho_e c_p \kappa} \tag{4}$$

where:
- η_H – current efficiency of gas emission,
- h – the inter-electrode gap height,
- k_H – hydrogen electrochemical equivalent,
- μ_e – the electrolyte dynamic viscosity,
- a, a_T – thermal diffusivity coefficient in laminar and turbulent motion [7,8],
- ρ_e, ρ_H – density of the electrolyte, hydrogen,
- c_p – specific heat of the electrolyte,
- κ – electrolyte conductivity.

Equations (1-4) should satisfy the following boundary conditions for:

- flow rate

  $v_x, v_y = 0$ for $y = 0$,

  $v_x = A_p\omega_p \cos\omega_p t$ $v_y = \frac{\partial h}{\partial t}$ for $y = h$,

- pressure

  $p = p_z$ for $x = x_z$,

- temperature:

  – on the walls: $T = T_s$ for $x \geq x_w$ *i* $y = 0$ and $y = h$

  – on the inlet $T=T_w$

  where: x_z – coordinate of the interelectrode gap end,

  T_s – temperature of electrodes, T_w – temperature on the inlet.

2.1. Motion equation integrals

Having introduced dimensionless quantities defined by formulas:

$$\tilde{x}=\frac{x}{L_0},\quad \tilde{y}=\frac{y}{h_0},$$

$$\tilde{v}_x=\frac{v_x}{v_0},\quad \tilde{v}_y=\frac{v_y}{v_0}\frac{R_0}{h_0},\quad \tilde{p}=\frac{p h_0}{\mu_e v_0}\frac{h_0}{L_0}$$

motion equations, describing flow of the electrolyte and oxygen compound, can be presented in the form:

$$\lambda(\tilde{v}_x \frac{\partial \tilde{v}_x}{\partial \tilde{x}} + \tilde{v}_y \frac{\partial \tilde{v}_x}{\partial \tilde{y}}) = -\frac{\partial \tilde{p}}{\partial \tilde{x}} + \frac{\partial^2 \tilde{v}_x}{\partial \tilde{y}^2} \tag{5}$$

$$\frac{\partial \tilde{v}}{\partial \tilde{y}} = 0 \tag{6}$$

Quantities denoted by index 'zero', are mean quantities within the considered flow area, $\lambda = Re\frac{h_0}{L_0}$ - Reynold's modified number.

In motion equation (5) Reynold's modified number is the system small parameter. Thus, its solution can be found in the form of a power series in relation to λ in the form:

$$v_x = \sum_{i=0}^{\infty} \lambda^i v_x^i \quad v_y = \sum_{i=0}^{\infty} \lambda^i v_y^i \quad p = \sum_{i=0}^{\infty} \lambda^i p^i \tag{7}$$

Substituting series (7) into equation motion (5), and the flow continuity equations (1), ordering and grouping expressions in relation to the same powers λ, for linear approximation in a dimensional form, the following sequence of equations can be obtained:

$$\frac{\partial(\rho_e v_x^0)}{\partial x} + \frac{\partial(\rho_e v_y^0)}{\partial y} = 0 \tag{8}$$

$$\frac{\partial(\rho_H v_x^0)}{\partial x} + \frac{\partial(\rho_H v_y^0)}{\partial y} = j\eta_H k_H h^{-1} \tag{9}$$

$$0 = -\frac{\partial p^0}{\partial x} + \mu_e \frac{\partial^2 v_x^0}{\partial y^2} \tag{10}$$

$$\frac{\partial(\rho_e v_x^1)}{\partial x} + \frac{\partial(\rho_e v_y^1)}{\partial y} = 0 \tag{11}$$

$$\rho_e\left(v_x^0 \frac{\partial v_x^0}{\partial x} + v_y^0 \frac{\partial v_x^0}{\partial y}\right) = -\frac{\partial p^1}{\partial x} + \mu_e \frac{\partial^2 v_x^1}{\partial y^2} \tag{12}$$

Boundary conditions are now in the form:

$$\begin{aligned} &v_x^0 = 0,\ v_y^0 = 0, \\ &v_x^1 = 0,\ v_y^1 = 0, \quad \text{for } y = 0 \end{aligned} \tag{13}$$

$$\begin{aligned} &v_x^0 = A_p \omega_p \cos\omega_p t\ ,\ v_y^0 = \frac{\partial h}{\partial t}, \\ &v_x^1 = 0,\ v_y^1 = 0, \quad \text{for } y = h \end{aligned}$$

$$p^0 = p_z \qquad p^1 = 0 \qquad \text{for } x = x_z \tag{14}$$

Having solved the obtained sequences of equations (8 ÷ 12), and using boundary conditions (19) and (20), we obtain the field of velocity and pressure, respectively:

$$v_x = \frac{6Q}{h^3}(hy - y^2) - \frac{13}{70}\frac{\rho_e}{\mu_e}\frac{QV}{h^2}(hy - y^2) + \frac{1}{10}\frac{\rho_e}{\mu_e}\frac{QV}{h^6}(21hy^5 - 12y^6 - 10h^2y^4 + h^5y) \tag{15}$$

$$v_y = \frac{V}{h^3}(3hy^2 - 2y^3) - \frac{1}{\rho_e}\frac{\partial}{\partial x}\frac{\rho_e^2}{\mu_e}\left[\frac{13}{420}(2y^3 - hy^2) - \frac{1}{2100}(420h^2y^5 - 735hy^6 + 360y^7 - 110h^5y^2)\right] \tag{16}$$

$$p = \frac{12\mu Q}{h^3}(x - x_g) + \frac{13}{35}\frac{\rho_e Q V}{h^2}(x - x_g) \tag{17}$$

In order to account for a turbulent flow through the interelectrode gap, in an orthogonal coordinate system, dependencies describing distributions of the rate, have been accepted:

$$v_x = v_{xmax}\left[1 - \left|\frac{h-2y}{h}\right|\right]^{\frac{1}{n}} \tag{18}$$

$$v_y = V\left(\frac{2y}{h}\right)^{\frac{n+1}{n}} \tag{19}$$

where: $v_{xmax} = \frac{n+1}{n}\frac{Q}{bh}$ maximum longitudinal flow rate in the cracks cross-section when the Q volume flow is represented by [$\frac{m^3}{s}$]

Values of Reynold's number *Re*, for which there occurs transition from laminar into turbulent flow (Re_{kr} = 2500) [3], can be determined from the formula:

$$Re = \frac{v_{śr}\,4r_h}{\nu}, r_h = \frac{bh}{2(b+h)}, \quad v_{śr} = \frac{Q}{hb}, \quad \nu = \nu_e(1 + 2.5\beta) \;\; \beta << 1.$$

Distribution of volume fracture β is determined from the balance of hydrogen mass, produced on the cathode:

$$\frac{\partial}{\partial x}\left(\frac{p}{T}\beta\right) = \frac{\eta_H \kappa_H R}{\mu_H Q} j \tag{20}$$

where:

$\rho_{Ho} = \frac{\mu_H p}{RT}$ – hydrogen density,

R – gas constant,

μ_H – dynamic hydrogen viscosity.

2.2. Equation of the shape evolution

Equation of the surface electrochemical dissolution in the direction of *Y* axis of the *XYZ*- sytem related to the anode for the considered case, is defined by dependence [5]:

$$\frac{\partial Y_A}{\partial t} = k_v \kappa_0 \Phi_{TG}^{-1}\frac{U-E}{h}\sqrt{1 + \left(\frac{\partial Y_A}{\partial X}\right)^2 + \left(\frac{\partial Y_A}{\partial Z}\right)^2} \tag{29}$$

$$\Phi_{TG} = \frac{1}{h}\left[\int_0^h \frac{dy}{(1+\alpha_T(T-T_0))(1-\beta)^{3/2}}\right] \tag{30}$$

where:

k_v – electrochemical machinability coefficient,

α_T – temperature coefficient of electrical conductivity,

κ_o – the medium conductivity.

2. Numerical model

Determination of the machined surface shape evolution Has been described by equation (29) defining the real change of the machined surface shape.

The machined surface initial shape and the tool electrode were defined in 3D CAD program as free surfaces of NURBUS type.

For numerical calculations, discretion of MS and TE was made through the surface approximation by curves. In this way, a set of curve pairs TE_k, MS_k was obtained which next were described by points, in a global coordinate system , with assigned accuracy (Fig. 2).

$$x_i = \sum_{i=1}^{i} \Delta x_i \tag{31}$$

where: $i = 0, 1, 2 \ldots I$

After having performed discretion of TE and WP surfaces, the work piece shape evolution equation was solved with the use of successive approximation method, applying the method of time steps according to the algorithm (Fig. 2a).

a)

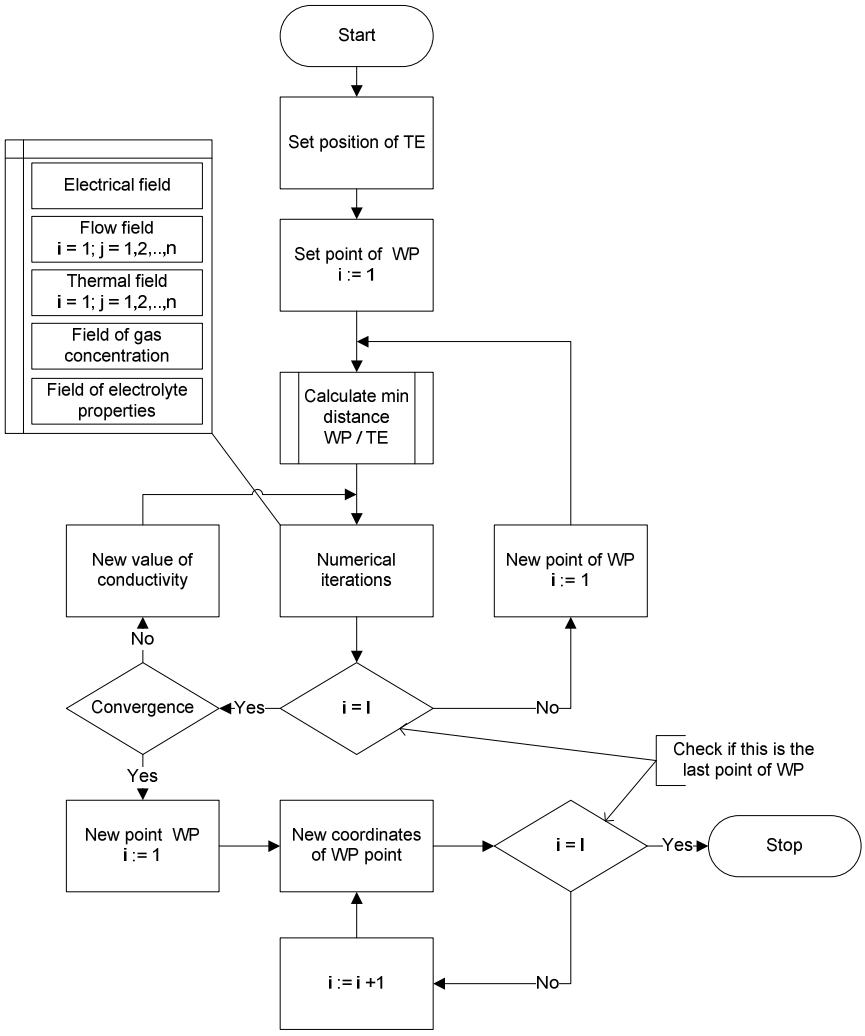

b)

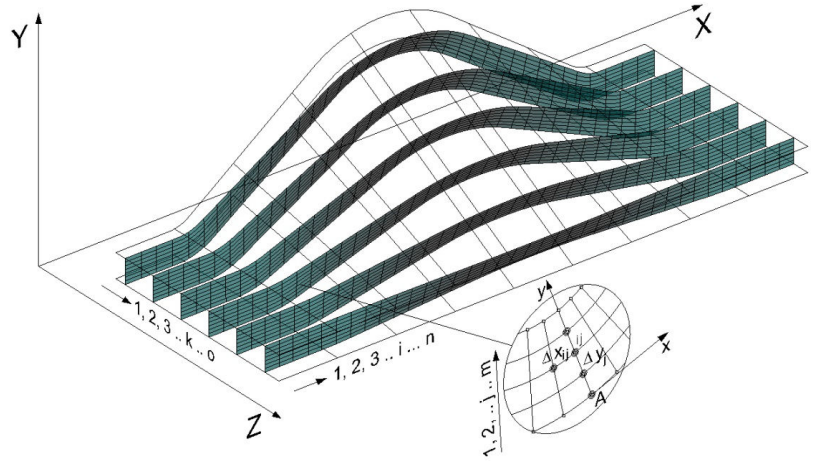

Fig. 2. ECM numerical model: a) algorithm for solving equations describing the process (l, i - current and last points of WP describing curve), b) IEG digitization

Time t has been presented by means of a set of points:

$$t_k = t_0 + k\,\Delta t \tag{32}$$

where: $k = 0, 1, 2, ... K$

The sequence of calculations is carried out here with the gap thickness distribution, "frozen" for a given time step.

In case of shape surfaces calculating the minimal WP and TE distances is a complex process. It's caused by the fact that analysis of a given WP point should be conducted accordingly with the TE points that are in the vicinity with the considered point, in all possible directions of 3D plane. To optimize the calculations a matrix of all points laying on TE over the considered WP point is created (Fig. 3). A sequence of these actions is shown on a diagram (Fig. 3).

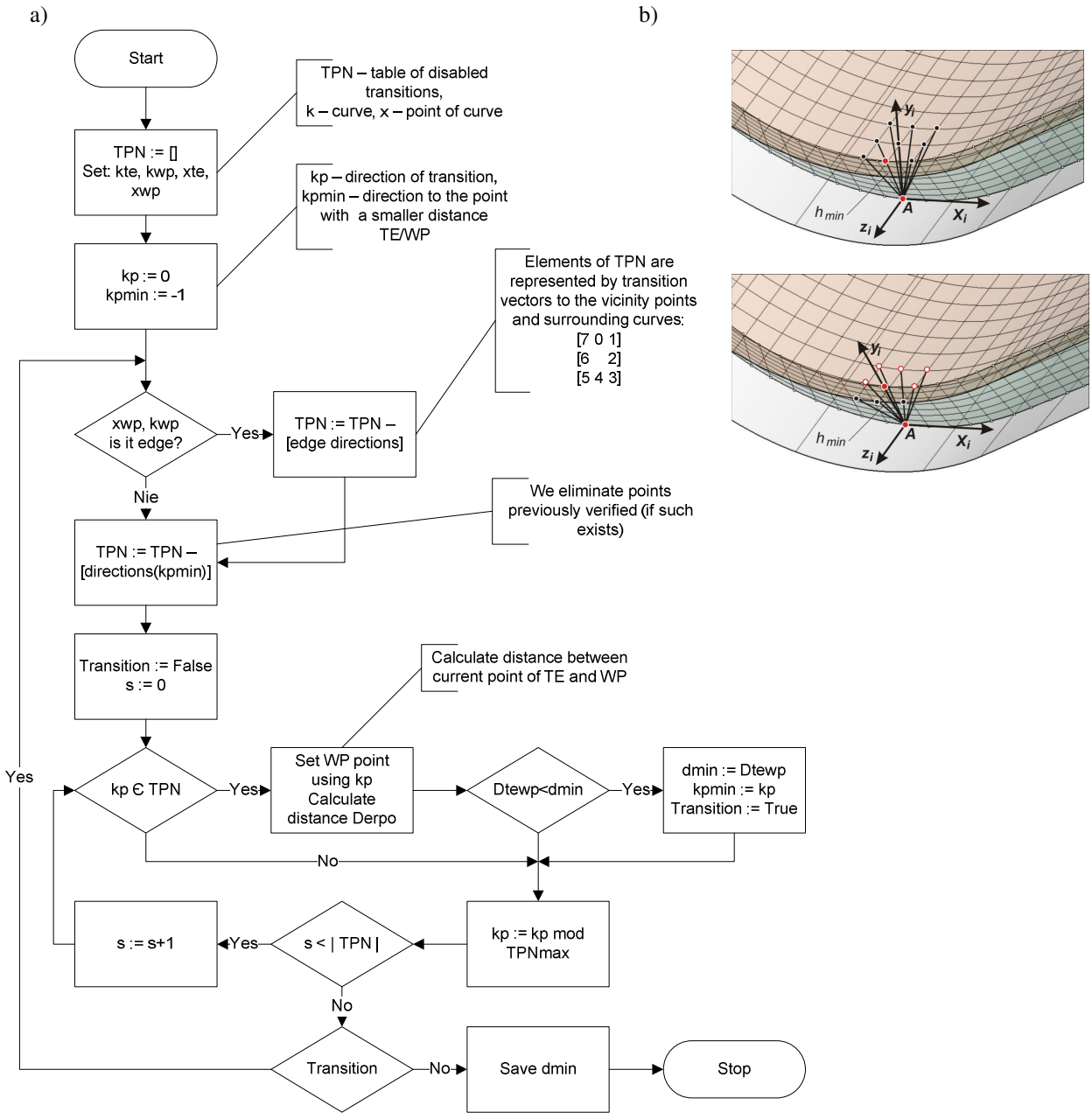

Fig. 3. Designing a minimal distance of the electrodes: a) h_{min} designing algorithm, b) momentary point matrixes

Symbols for Fig. 3:

kp	- variable representing transition direction to the neighborhood point,
Dtewp	- distance between points defined by transition kp for TE and WP points,
Transition	- variable to carry on information “point with a smaller distance discovered”,
TPNmax	- constant value representing number of neighborhood points equal 9,
s	- work variable used to index table elements
TPN	- power of TPN represents number of points to verify if is closer.

Figure 3 demonstrates a scheme of time steps for composition of the tool electrode two vibrating motions:

- longitudinal vibrations (main *Y*-axis direction) – with vibration frequency f_w and vibration amplitude A_w, performed in the direction of the main move,

- transverse vibrations (X-axis direction) – with vibration frequency f_p and vibration amplitude A_p , performed along X axis within the plane, perpendicular to the main motion direction.

Vibration frequency of $f_w = 4f_p$ was assumed, no phase shift for $\phi_w = 0$ amplitudes.

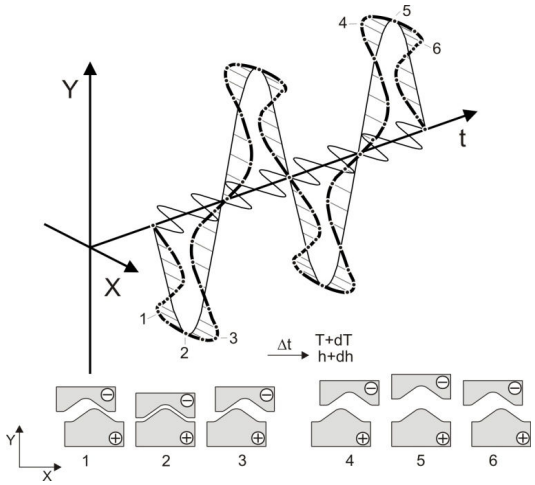

Fig. 4. Scheme of time step

Such a shift of vibration amplitudes in relation to each other provides a symmetrical, resultant motion of TE in relation to the main vibrations with extreme deflections. This case is very advantageous in terms of ECM machining accuracy. In Fig. 5 examplary vibrations for different synchronizations are shown. It can be noted here that in extreme positions the resultant motion of the tool electrode results in different deflection of the tool electrode motion path in relation to the main vibrations. It has a direct influence on the conditions in SM and in result on the processing precision.

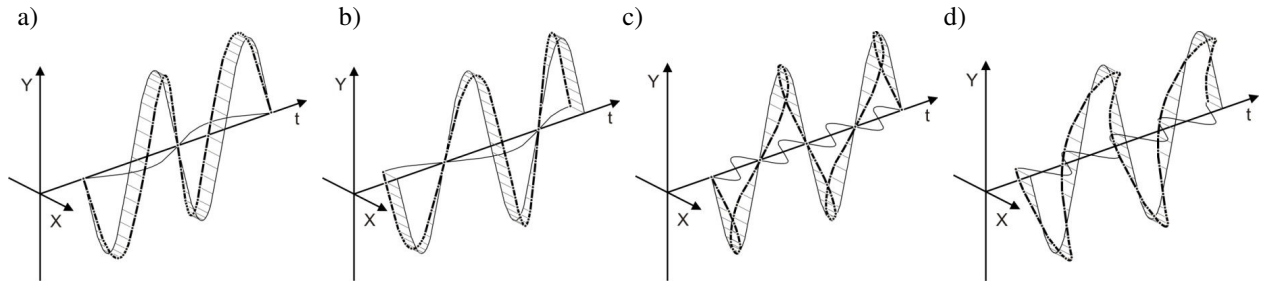

Fig. 5. Longitudinal and transverse vibrations compound : a) ½ $f_p = f_w$, $\phi_w = 0$, b) ½ $f_p = f_w$, $\phi_w = \pi/2$, c) 2 $f_p = f_w$, $\phi_w = 0$, d) 2 $f_p = f_w$, $\phi_w = \pi/2$

3. CONCLUSIONS

The calculations have been performed for shaping electrodes with geometric features presented in Fig. 5. Also, there have been shown sections along and across the interelectrode gap, for which calculation results are depicted in charts. This is a curvilinear surface, curved also in the direction of z axis. Viewing the issue as being flat involves seeking planes for performing calculations, defined as planes normal to the anode surface though, at the same time, limited by the electrode surfaces. The assumption is that the feed system provides a constant flow rate in IEG. Calculations had been performed until a quasi-stationary state was reached, i.e. the state for which thickness of MP and physical conditions between the electrodes changes occur periodically.

Machining parameters of more importance have been presented in calculations:

- initial gap - 0.2 mm,

- velocity of sliding motion of TE - 0.0125 mm/s,
- interelectrode voltage - 15 V,
- parameters of longitudinal vibrations A_w=0.1 mm, f_w=25 1/s,
- parameters of transverse vibrations A_p=0.05, f_p=100 1/s.

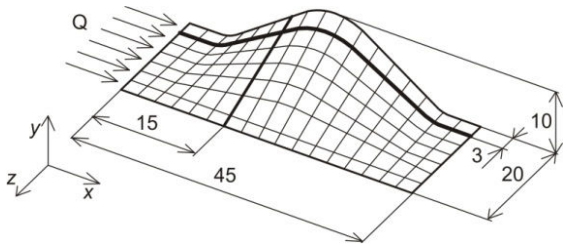

Fig. 6. The geometrical features of electrodes

Distributions of T temperature for a chosen section are presented in Fig. 7 as well as velocities V_x (Fig. 7b) along the gap thickness. Initial course of these distributions results from the laminar electrolyte flow next from the turbulent electrolyte flow.

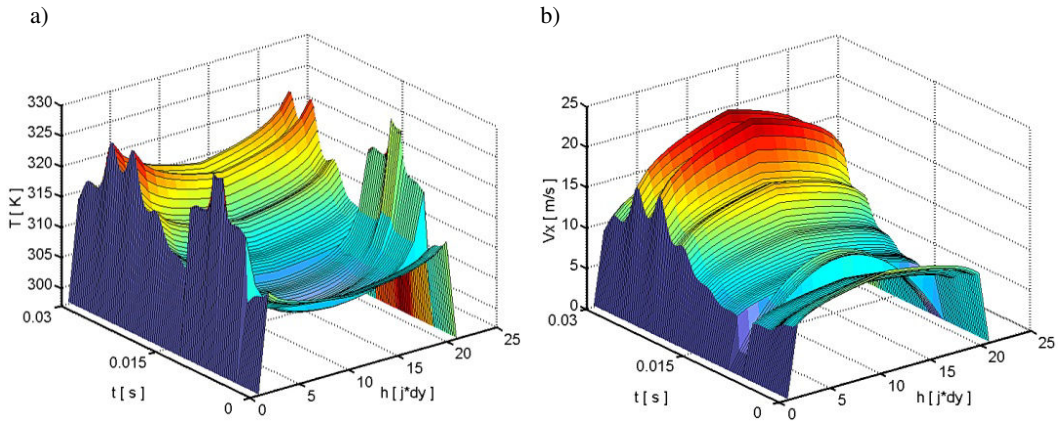

Fig. 7. Distribution along thickness: a) temperature, b) velocity of flow electrolyte

In charts (Fig. 8) there are presented distributions of p pressure, mean flow rate of the electrolyte v_{mean}, current density j and gap thickness IE h along the interelectrode gap. The periodic changes for distribution along thickness IEG for temperature and velocity of flow electrolyte are shown in Fig. 8.

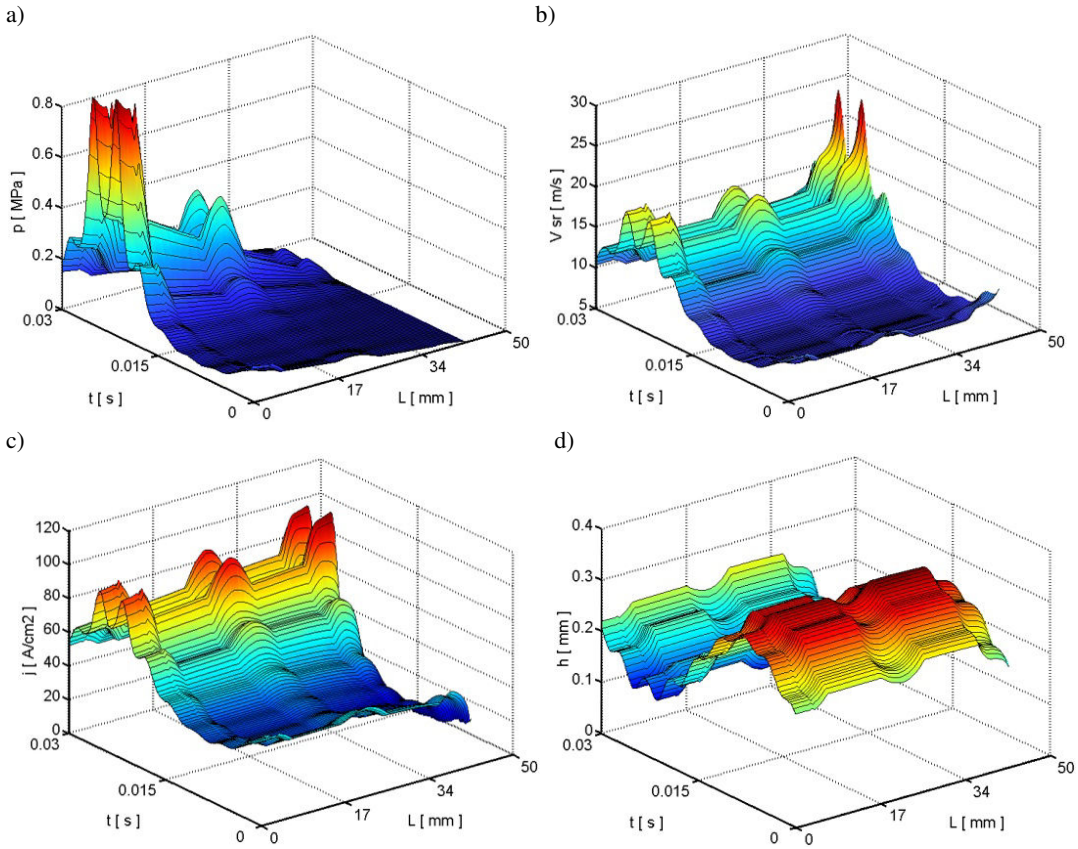

Fig. 8. Distribution along SM: a) pressure p, b) velocity of flow electrolyte Vśr, c) current density d) crack height IEG h

In addition, an analysis of the average current density for a portion of the longitudinal vibration period was performed, where the processing takes place most intensively (Fig. 9). The analysis was performed for the symmetric vibration system: 1 - ½ $f_p = f_w$, $\phi_w = 0$, 2 - $f_p = f_w$, $\phi_w = \pi/2$, 3 - $2f_p = f_w$, $\phi_w = 0$, 4 - 4 $f_p = f_w$ $\phi_w = 0$.

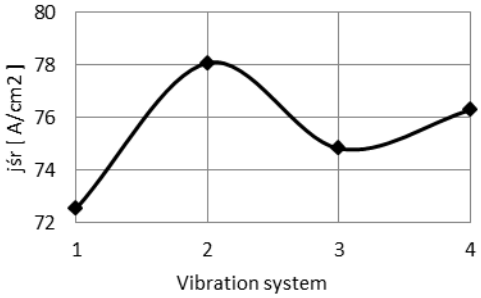

Fig. 9. Average current density for selected systems synchronize oscillations

The received calculation results confirm the expected quality change courses of chosen parameters:

- method of synchronize the vibrations affect the average values of current density,
- induction of the tool electrode vibrations case the profile deformation of the electrolyte flow rate along thickness IEG which additionaly influences the electrolyte temperature change near the vibrating wall (Fig. 7),
- deformation of the electrolyte flow rate profile along IEG thickness grows along with the electrode vibration frequency increase. Thus, there are certain boundary values of vibration

frequencies and amplitudes for which there will occur the phenomenon of the electrolyte reversal in IEG,
- the electrolyte turbulent flow in the gap results in flattening the profile of the electrolyte flow rate which has a direct influence on temperature distribution along the interelectrode gap,
- local thicknesses of the inter-electrode gap (Fig. 8d) undergo changes. This has an impact on the variability of electrochemical dissolution velocity and inclination angle of the tool electrode profile in relation to the machining direction and electrode vibrations synchronization (Fig. 5) non-uniform distribution of the interelectrode gap thickness largely affects the distribution of pressure and the electrolyte flow rate (Fig. 7a-b),
- the mathematic model indicates that the gas phase concentration and the electrolyte temperature has an influence on variability of physical conditions along the flow (Fig. 7 c-d). These factors affect the change of such physical quantities as: the electrolyte viscosity, density, conductivity, and in consequence the electrochemical dissolution and machining accuracy.

In case when electrode vibrations are used it seems to be necessary to create mathematical models of ECM for the purpose of an optimal choice of the process parameters. Apart from the choice of amplitudes and vibration frequencies, their mutual synchronization is of special importance. Further simulation and experimental tests will allow for quantitative verification of the accepted mathematical model.

References

[1] Dąbrowski, L., Paczkowski, T., *Computer simulation of two-dimensional electrolyte flow in electrochemical machining*, Russian Journal of Electrochemistry, vol. 41, No. 1, 2005, pp. 91-98.

[2] Dąbrowski, L., *Podstawy komputerowej symulacji kształtowania elektrochemicznego*, Prace Naukowe, Mechanika z. 154, Wydaw. Politechniki Warszawskiej, Warszawa, 1992.

[3] Gryboś, R., *Podstawy mechaniki płynów*, PWN Warszawa 1998.

[4] Kiciak, P., *Podstawy modelowania krzywych i powierzchni*, Zastosowania w grafice komputerowej, Wyd. 1. WNT, Warszawa 2000.

[5] Kozak, J., *Kształtowanie powierzchni obróbką elektrochemiczną bezstykową (ECM)*, Prace Naukowe PW, Mechanika nr 41, Wydawnictwo Politechniki Warszawskiej, Warszawa. 1976.

[6] Kozak, J., *Mathematical models for computer simulation of electrochemical machining process*, Journal of Materials Processing Technology, Vol. 76, 1976.

[7] Kozak, J., *Komputerowe wspomaganie technologii drążenia elektrochemicznego*, SNOE nr 5, Warszawa 1999.

[8] Kozak, J., *Computer simulation system for electrochemical shaping*, J. Mater. Process. Technol. 109, 354–359, 2001.

[9] Łubkowski, K., *Stany krytyczne w obróbce elektrochemicznej*, Prace naukowe, Mechanika, z.163, Oficyna Wydawnicza PW, Warszawa, 1996.

[10] Paczkowski, T., Sawicki J., *Analysis of influence of physical conditions inside interelectrode gap on work piece shape evolution*, Engineering Mechanics, vol. 13, 2006, No. 2, p. 93-100.

[11] Paczkowski T., Sawicki, J., *Electrochemical machining of curvilinear surfaces*, (MST410/07), Journal of Machining Science and Technology, 2008 USA.